Recent inter-annual trend of spherical aerosol in East Asia based on integrated analysis of remote sensing and a chemical transport model

Yukari Hara* , Itsushi Uno
Research Institute for Applied Mechanics, Kyushu University, Kasuga Park 6-1, Kasuga, Fukuoka, Japan

Atsushi Shimizu, Nobuo Sugimoto, Ichiro Matsui, Toshimasa Ohara
National Institute for Environmental Studies, Tsukuba, Ibaraki, Japan

Shuichi Itahashi
Department of Earth System Science and Technology, Kyushu University, Kasuga, Fukuoka, Japan

1. INTRODUCTION

Recent rapid economic growth of eastern Asian countries has caused a marked increase of anthropogenic emission (Ohara et al., 2007) since 2000. However, Lu et al. (2011) reported that SO_2 emission in China decreased by 9.2% from 2006 to 2010 due to the wide application of flue-gas desulfurization (FGD) devices in power plants. On the other hand, Lamsal et al. (2011) showed that NOx emission from eastern Asia increased by 18.8 % during 2006-2009. Anthropogenic emission in eastern Asia has changed dramatically by the balance between economic development and political emission control.

National Institute for Environmental Studies (NIES) has been constructing a ground-based network of automated dual-wavelength (532, 1064 nm), polarization-sensitive (532 nm) Mie-lidar systems to examine air quality continuously in eastern Asia since 2001 (Shimizu et al., 2004). In this paper, recent annual trend of anthropogenic aerosol loading during 2004-2011 was investigated using ground-based lidar data, space-borne lidar, airport visibility data, the Moderate resolution Imaging Spectroradiometer (MODIS) data and the Community Multi-scale Air Quality Modeling System (CMAQ) chemical transport model simulation.

2. 2. Model description and Observations

Transport of air pollutants was simulated using a modeling system (CMAQ ver. 4.4) released by the US EPA (Byun and Ching, 1999). The meteorological fields were obtained from the Regional Atmospheric Modeling System (RAMS) version 4.3 (Pielke et al., 1992) with initial and boundary conditions defined by NCEP reanalysis data (2.5° resolution and 6 h interval). The horizontal model domain for the CMAQ simulation is 6240×5440 km^2 on a rotated polar stereographic map projection centered at 25°N, 115°E with 80×80 km^2 grid resolution (see Fig.1). For vertical resolution, 14 layers are used in the sigma-z coordinate system up to 23 km, with about seven layers within the boundary layer below 2km. The SAPRC-99 scheme (Carter et al., 2000) is applied for gas-phase chemistry (with a number of 72 chemical species and 214 chemical reactions, including 30 photochemical reactions), and the AERO3 module for aerosol calculation. Anthropogenic emission data were obtained from the Regional Emission Inventory in Asia (REAS) (Ohara et al., 2007). Using the method proposed by Malm et al. (1994), the extinction coefficient (b_{ext}) at 550 nm by CMAQ was calculated for black carbon (BC), organic carbon (OC), sulfate, and nitrate.

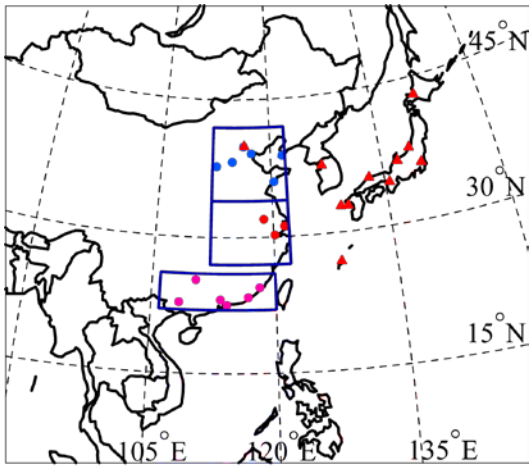

Fig. 1. Model domain and analysis region. Circles indicate airport stations, and Triangles indicate NIES lidar stations.

**Corresponding author:* Yukari Hara, Research Institute for Applied Mechanics, Kyushu University, Kasuga Park 6-1, Kasuga, Fukuoka, Japan; e-mail: yhara@riam.kyushu-u.ac.jp

Mie-scatter Lidar is a powerful method for measuring the vertical structure of dust and pollutants. We used nine Lidar sites data from the NIES ground-based Lidar network, which provide long-term vertical profiles of aerosols with high spatial and temporal resolution (see Fig. 1). The extinction coefficient is derived based on the Fernald's method (Fernald 1984) by setting a boundary condition at 6 km and S1 = 50 sr. Aerosol extinction coefficient is separated into 'dust extinction' and 'spherical particles extinction' using particle depolarization ratio. The spherical component was analyzed in this study.

We also used CALIOP Level 2 Ver. 3.01 data (Winker et al. 2007, 2010) to derive spherical aerosol extinction coefficient using the particle depolarization ratio and particle extinction coefficient.

Airport visibility data was used to investigate surface air quality in China. The data was downloaded from Wyoming university web server (http://weather.uwyo.edu/surface/meteogram/). Uncorrected extinction coefficient is calculated via the Koschmieder relationship (Koschmieder, 1926)

$$b_{ext} = 1.9/V \quad (1)$$

where V is visibility (km). To remove the natural events such as precipitation, dust, fog, mist and gale, the present weather code by SYNOP were used. Visibility data were also screened when the relative humidity is higher than 90 %.

MODIS level 3 collection 5.1 products provide the aerosol optical depth (AOD) at 550 nm and the fine-mode fraction (Remar et al. 2005). We derived the fine-mode AOD by multiplication of aerosol optical depth and fine-mode fraction.

3. RESULTS

The prime motivation of this study is to clarify the recent trend of spherical aerosol loading over eastern Asia basically based on the optical observations during 2004-2011. We will show the trend at NIES ground lidar stations and the regional difference over eastern Asia in section 3.

3.1 Long-term trend of spherical aerosol at NIES ground lidar stations

Figure 2 shows the long-term variation of spherical monthly averaged AOD based on the ground/space lidar measurements, MODIS and CMAQ at (a) Beijing, (b) Hedo and (c) Tsukuba. To evaluate the trend of spherical AOD, time regression model based on least squares was used to the temporal variation in the concentration. We separated our analysis period into period A (2004-2008) and B (2008-2011).

$$C(t) = \alpha + \beta t + \gamma \sin(2\pi t/12 + \phi) \quad (2)$$

where t denotes time in months. Model parameters α, β, γ and ϕ represent intercept, slope of an annual trend, annual cycle-amplitude, and phase-angle of an annual cycle. Second term shows the long-term trend, and third term shows the seasonal variation. Estimates of model parameters in Eq. 2 are summarized in Table 1 for each stations.

The significance of an annual trend was evaluated by testing the null hypothesis H_0: $\beta=0$, against the alternative hypothesis H_1: $\beta\neq0$; the significance level used in this analysis is 5%.

From the results of Table 1, different optical measurements almost showed the consistent trends. Spherical AOD had increased significantly from 2004-2008 at all stations. After 2008, spherical AOD had decreased at downwind stations, Hedo and Tsukuba, while positive trend was still discernible at Beijing.

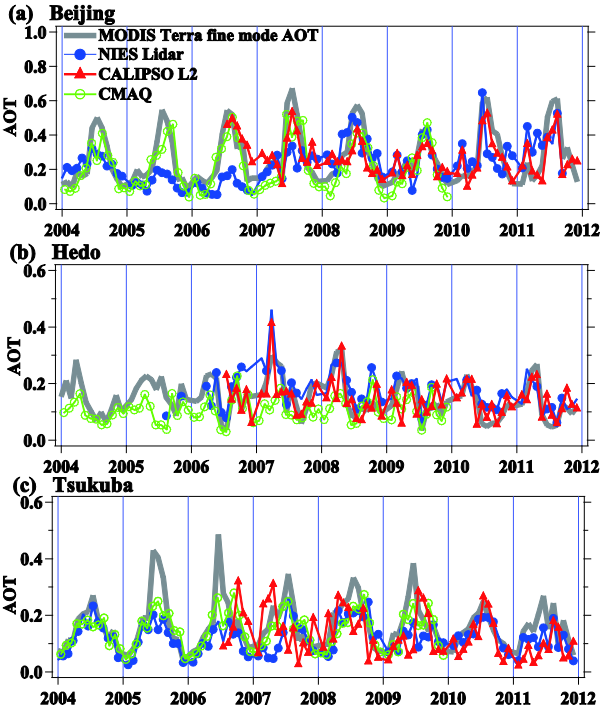

Fig. 2. Temporal variation of monthly averaged spherical AOD at (a) Beijing, (b) Okinawa/Hedo, (c) Tsukuba.

Table 1 Regression parameters in Eq. (2) based on monthly AOD at NIES lidar stations.

Region	parameters / period / obs.	α		β		γ	
		2004-2008	2008-2011	2004-2008	2008-2011	2004-2008	2008-2011
Beijing	NIES	0.133	0.286	0.028*	0.003	0.056	0.069
	CALIOP	-	0.243	-	0.008	-	0.085
	MODIS	0.233	0.273	0.016*	0.002	0.183	0.185
Hedo	NIES	0.117	0.205	0.031*	-0.018*	0.063	0.038
	CALIOP	-	0.147	-	-0.004	-	0.038
	MODIS	0.148	0.162	0.005*	-0.012*	0.062	0.066
Tsukuba	NIES	0.113	0.157	0.006*	-0.014*	0.068	0.048
	CALIOP	-	0.166	-	-0.023*	-	0.060
	MODIS	0.163	0.192	0.005*	-0.013*	0.112	0.087

3.2 Long-term trend of surface visibility data in China

The monthly extinction coefficient derived from airport visibility data for the Chinese three region, (a) northern part, (b) middle part, and (c) southern part of China were showed in Figure 3. Error bar shows the positive (negative) gap between monthly maximum (minimum) value and average value. AOD data was also shown in Figure 3. Since visibility data shows different seasonal variation from AOD, we conducted the trend analysis for the AOD peak season in the each region. Table 2 summarized the model parameters in Eq. 2 based on visibility data and MODIS data.

From the results of Table 2, the surface extinction coefficients and satellite AOD showed significant increasing trend for the three region during period A (2004-2008). The northern part of China exhibited still increasing trend after 2008. The trend over southern part of China turned negative in recent period B (2008-2011). The trend in middle part of China was indiscernible.

3.3 Horizontal distribution of spherical aerosol trend in Eastern Asia

The horizontal distributions of the annual slope of spherical aerosol loading (Eq. 2, β) were displayed in Figure 4. Figure (a) and (c) show the trend by the various observations. Pixels show MODIS trend, circle markers show airport visibility trend, stars show ground-based lidar trend. Figure (b) shows the spherical AOD trend by CMAQ. We showed only statistically significant value by testing the null hypothesis.

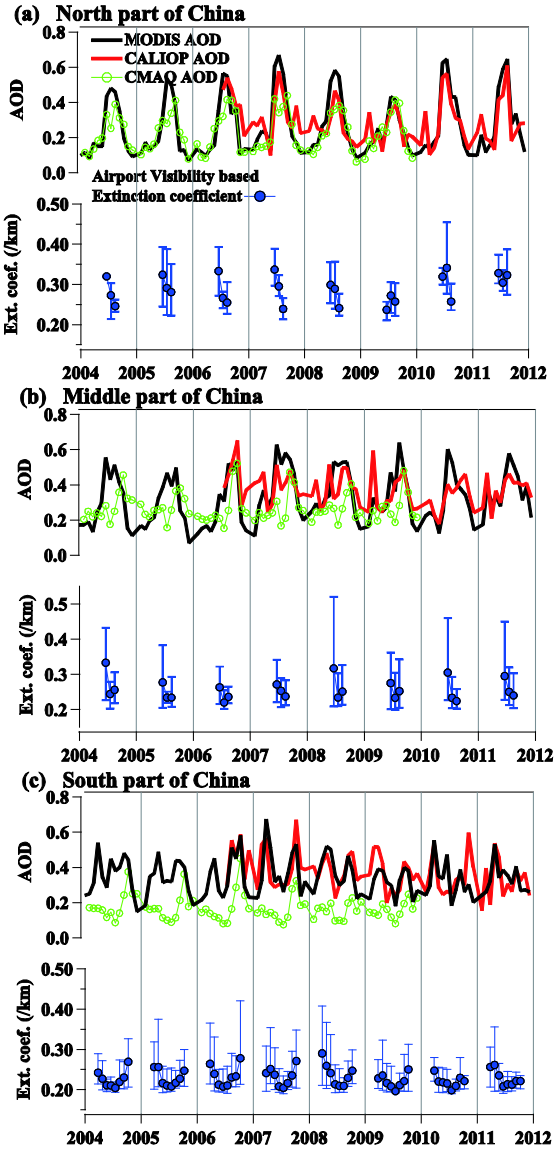

Fig. 3. Temporal variation of monthly averaged extinction coefficient and AOD at (a) north, (b) middle, (c) south part of China.

Table 2 Regression parameters in Eq. (2) based on visibility data and MODIS AOD for Chinese region.

Chinese Region	parameters / period / obs.	α		β		γ	
		2004-2008	2008-2011	2004-2008	2008-2011	2004-2008	2008-2011
North	Visibility	0.279	0.254	0.005*	0.015*	-0.036	-0.029
	MODIS	0.227	0.264	0.013*	0.004	0.199	-0.199
Middle	Visibility	0.302	0.305	0.001	0.001	-0.058	-0.068
	MODIS	0.267	0.350	0.020*	-0.005	0.174	-0.151
South	Visibility	0.235	0.240	0.003*	-0.001	-0.031	-0.030
	MODIS	0.343	0.356	0.003*	-0.006*	-0.113	-0.072

From the results of trend analysis based on observations, the significant positive trends were exhibited over the wide range of eastern Asia during the period A (Fig. 4a). On the other hand, the trends turned negative over the southern Chinese region and downwind region in the period B. The trends of northern part of China showed significant positive (Fig. 4c).

CMAQ positive trend over the downwind region during period A is almost consistent with the optical measurement (Fig. 4b). Emission inventory used in the simulation considered the increased energy consumption in eastern Asia from 2004-2006. Therefore CMAQ results suggested that the positive trends of spherical aerosol loading observed by optical remote sensing were mainly caused by the increase of anthropogenic emission.

Katsuno et al (1996) showed that sulfate aerosol is the dominant component of airborne suspended particulate matter based on the ion analysis at mountain station of Japan. Lu et al. (2011) reported that SO_2 emission in China decreased by 9.2% from 2006 to 2010 due to the wide application of flue-gas desulfurization (FGD) devices in power plants. Therefore the recent decrease trend of spherical aerosol loading in downwind region may be basically caused by the SO_2 emission reduction due to the FGD devices in China. On the other hand, Lamsal et al. (2011) showed that NOx emission from East Asia increased by 18.8 % during 2006-2009. Thus, the AOD increase trend in northeastern China might be attributed by increase of secondary aerosol formed from precursor species including NOx after 2008.

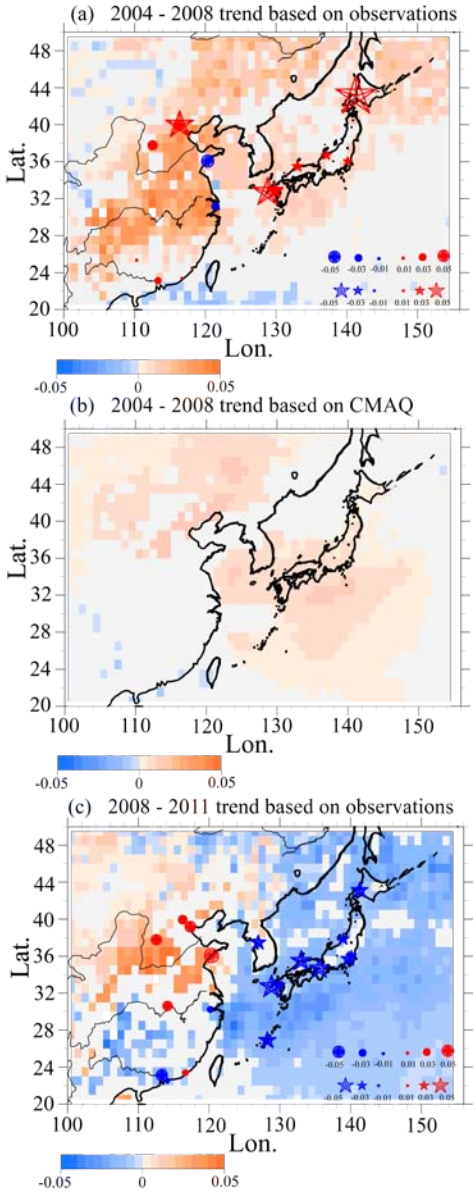

Fig. 4. Horizontal distributions of the trends (β in Eq. 2) based on observations (a) , (c) and CMAQ (b). Pixels in (a) and (c) indicate the trend based on MODIS AOD, the circles show the trend based on visibility data, the stars show the trend based on NIES lidar AOD.

4. Conclusions

The recent trend of spherical aerosol loading in eastern Asia during 2004-2011 was investigated using ground-based lidar data, space-borne lidar, airport visibility data, the Moderate resolution Imaging Spectroradiometer (MODIS) data and the Community Multi-scale Air Quality Modeling System (CMAQ) chemical transport model simulation. Results of our analyses clarified the following points.

Various optical measurements clarified that the spherical AOD had increased significantly for the period between 2004-2008. After 2008, the measurements showed that the spherical AOD exhibited significant decrease trend in southern part of China and downwind region. The positive trends were observed only in northern part of China. Since the main composition of spherical aerosol around Japan is sulfate, the recent AOD decrease trend in downwind region may be basically caused by the SO_2 emission reduction due to the FGD devices in China. The AOD increase trend in northeastern China might be attributed by increase of secondary aerosol formed from precursor species including NOx after 2008.

5. Acknowledgements

This work was partly supported by the Global Environment Research Fund of the Ministry of Environment, Japan (S-7) and the Joint Research Fund of Research Institute for Applied Mechanics, Kyushu University. The authors thank NASA Langley Research Center Atmospheric Sciences Data Center providing CALIPSO data and the MODIS Atmosphere Discipline Group for providing the MODIS data.

6. References

Byun, D. W. and J. K. S. Ching, 1999 : Science Algorithms of the EPA Models-3 Community Multi-scale Air Quality (CMAQ) Modeling System. NERL, Research Triangle Park, NCEPA/600/R-99/030.

Carter, W. P. L., 2000: Documentation of the SAPRC-99 chemical mechanism for VOC reactivity assessment, Final report to California Air Resource Board, Contract No. 92-329 and 95-308, May.

Fernald, F. G. , 1984 : Analysis of atmospheric LIDAR observations: Some comments. Appl. Optics, 23, 652-653.

Kanamitsu, M., W. Ebisuzaki, J. Woollen, S.-K. Yang, J. J. Hnilo, M. Fiorino and G. L. Potter, 2002: NCEP-DOE AMIP-II Reanalysis (R-2). Bull. Amer. Meteor. Soc., 83, 1631-1643.

Katsuno, T., H. Satsumabayashi, K. Sasaki, M. Shikano, M. Ota, S. Hatakeyama and K. Murano, 1996: Chemical components of airborne particulate matter and acid deposition in Happoone and Nagano city. J. Jpn. Soc. Atmos. Environ., 31, 282-291 (in Japanese).

Kurokawa, J. and T. Ohara, 2012: Recent trends for emission of air pollutants and greenhouse gases in Asia: Regional emission inventory in Asia (REAS) version 2. Third international workshop on emission inventory in Asia.

Lamsal, L. N., R. V. Martin, A. Padmanabhan, A. van Donkelaar, Q. Zhang, C. E. Sioris, K. Chance, T. P. Kurosu and M. J. Newchurch, 2011 : Application of satellite observations for timely updates to global anthropogenic NOX emission inventories. Geophys. Res. Lett., 38, L05810, doi:10.1029/2010GL046476.

Koschmieder, H., 1926 : Theorie der horizontalen Sichtweite Beit. Phys. Atmos., 12, 33– 55.

Lu, Z., Q. Zhang and D. G. Streets, 2011 : Sulfur dioxide and primary carbonaceous aerosol emissions in China and India, 1996-2010. Atmos. Chem. Phys., 11, 9839-9864.

Malm, W. C., J. F. Sisler, D. Huffman, R. A. Eldred and T. A. Cahill, 1994: Spatial and seasonal trends in particle concentration and optical extinction in the United States. J. Geophys. Res., 99, 1347−1370.

Ohara, T., H. Akimoto, J. Kurokawa, N. Horii, K. Yamaji, X. Yan and T. Hayasaka, 2007 : An Asian emission inventory of anthropogenic emission sources for the period 1980-2020 . Atmos. Chem. Phys., 7, 4419-4444.

Pielke, R. A., W. R. Cotton, R. L. Walko, C. J. Tremback, W. A. Lyons, L. D. Grasso, M. E. Micholls, M. D. Moran, D. A. Wesley, T. J. Lee and J. H. Copeland , 1992 : A comprehensive meteorological modeling system — RAMS . Meteor. Atmos. Phys., 49, 69-91.

Remer, L. A., Y. J. Kaufman, D. Tanré, S. Mattoo, D. A. Chu, J. V. Martins, R.-R. Li, C. Ichoku, R. C. Levy, R. G. Kleidman, T. F. Eck, E. Vermote and B. N. Holben, 2005: The MODIS

aerosol algorithm, products, and validation. J. Atmos. Sci., 62, 947−973.

Shimizu, A., N. Sugimoto, I. Matsui, K. Arao, I. Uno, T. Murayama, N. Kagawa, K. Aoki, A. Uchiyama and A. Yamazaki, 2004 : Continuous observations of Asian dust and other aerosols by polarization lidars in China and Japan during ACE-Asia . J. Geophys. Res. , 109 , D19S17, doi:10.1029/2002JD003253.

Shimizu, A., N. Sugimoto, I. Matsui, B. Tatarov, C. Xie, T. Nishizawa, and Y. Hara, 2008: NIES lidar Network; strategies and applications. 24th International Laser Rader Conference, 23-28 June 2008, Boulder, Colorado, USA, ISBN, 978-0-615-21489-4, 707-710.

Winker, D. M., W. H. Hunt and M. J. McGill, 2007: Initial performance assessment of CALIOP. Geophys. Res. Lett., 34 , L19803, doi:10.1029/2007GL030135.

Winker, D. M., J. Pelon, J. A. Coakley Jr., S. A. Ackerman, R. J. Charlson, P. R. Colarco, P. Flamant, Q. Fu, R. M. Hoff, C. Kittaka, T. L. Kubar, H. Le Treut, M. P. Mccormick, G. Mégie, L. Poole, K. Powell, C. Trepte, M. A. Vaughan and B. A. Wielicki, 2010: The CALIPSO mission: A global 3D view of aerosols and clouds. Bull. Amer. Meteor. Soc., 91, 1211−1229.